**OMTON, Volume *32***

## Supplemental information

# T cell receptor-directed antibody-drug conjugates for the treatment of T cell-derived cancers

**Katrin Schoenfeld, Jan Habermann, Philipp Wendel, Julia Harwardt, Evelyn Ullrich, and Harald Kolmar**

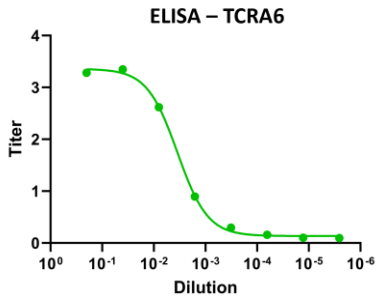


**Figure S1** Chicken immune response against TCRA6. Enzyme-linked immunosorbent assay (ELISA) for determination of final antibody titer in serum of immunized chickens. Experiment was conducted by Davids Biotechnologie GmbH (Regensburg, Germany).

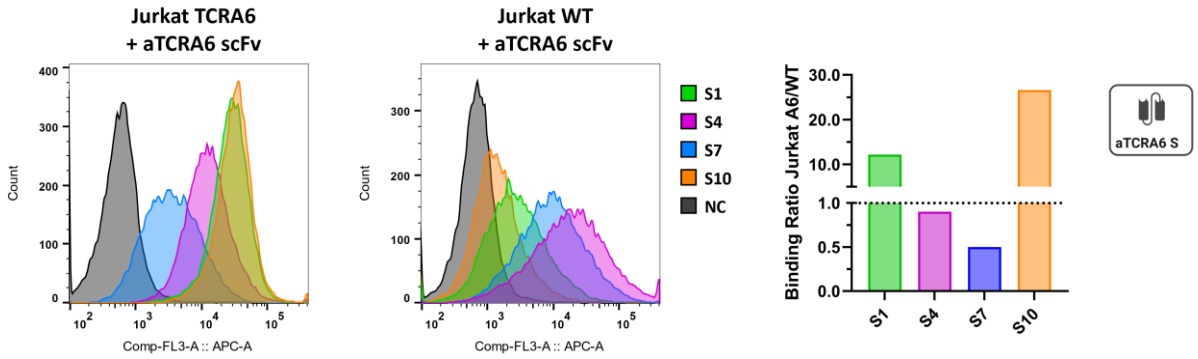


**Figure S2** Cellular binding of aTCRA6 scFvs. Flow cytometry analysis of Jurkat TCRA6 target and Jurkat WT off-target T cells incubated with 1000 nM of aTCRA6 scFv candidates S1, S4, S7, and S10, respectively. Negative controls without scFv incubation are shown in black. Staining was conducted *via* anti-his AF647-conjugated secondary detection antibody. Binding ratios of Jurkat TCRA6 to Jurkat WT cells were calculated by division of by normalized mean fluorescence values.

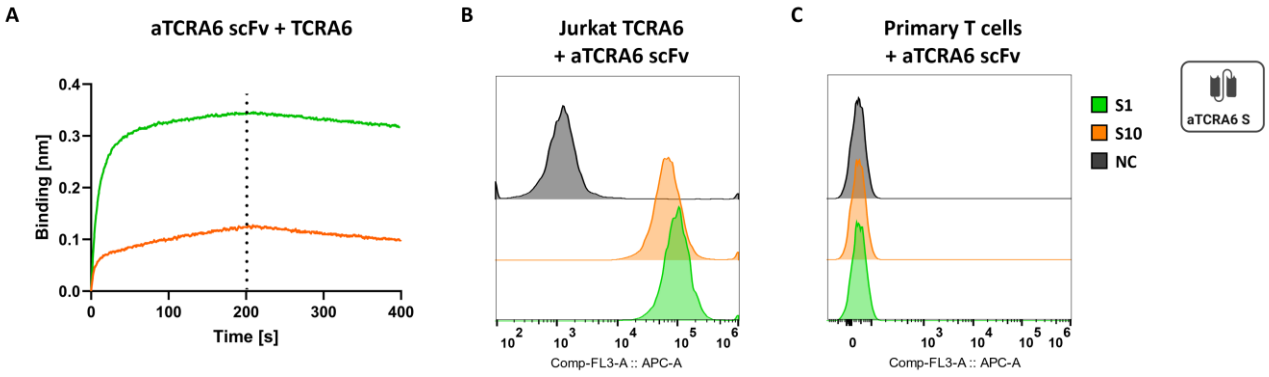


**Figure S3** Binding properties of aTCRA6 scFvs S1 and S10. (A) BLI measurement. Biotinylated TCRA6 was loaded onto SAX biosensor tips and associated with 500 nM aTCRA6 S1 and S10, respectively. (B) Target cell binding. Flow cytometry analysis of Jurkat TCRA6 target cells incubated with 1000 nM aTCRA6 S1 and S10, respectively. Staining was conducted using anti-his AF647-conjugated secondary detection antibody. (C) Off-target cell binding. Flow cytometry analysis of primary T cells isolated from human donor blood incubated with 1000 nM aTCRA6 S1 and S10, respectively. Staining was performed using mouse anti-his secondary antibody and anti-mouse IgG APC tertiary antibody for detection.

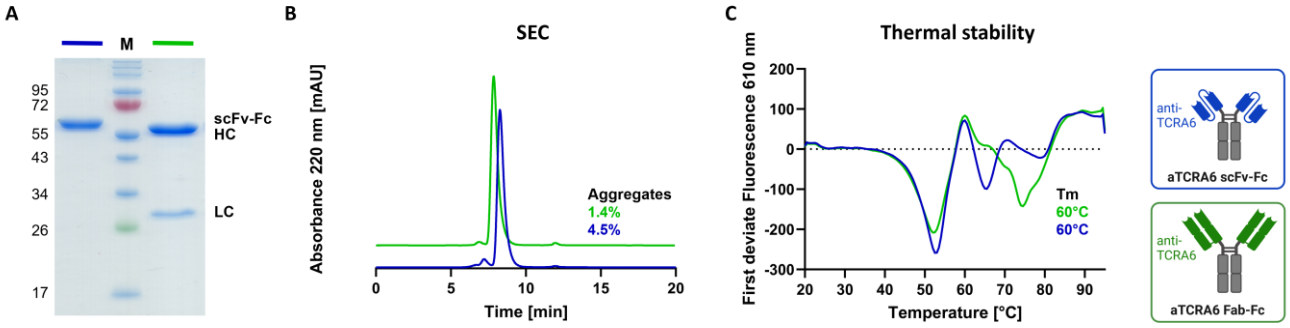


**Figure S4** Biophysical characterization of aTCRA6 scFv-Fc/Fab-Fc. (A) Reducing SDS-PAGE of depicted aTCRA6 antibodies. (B) Size exclusion chromatography. The percentages of aggregation were determined by integration of the absorbance peak areas. (C) Thermal shift assay. Thermal stability was analyzed using differential scanning fluorimetry with SYPRO Orange dye. Derivatives of melt curves and melting temperatures (Tm) were assessed using the BioRad CFX Maestro software.

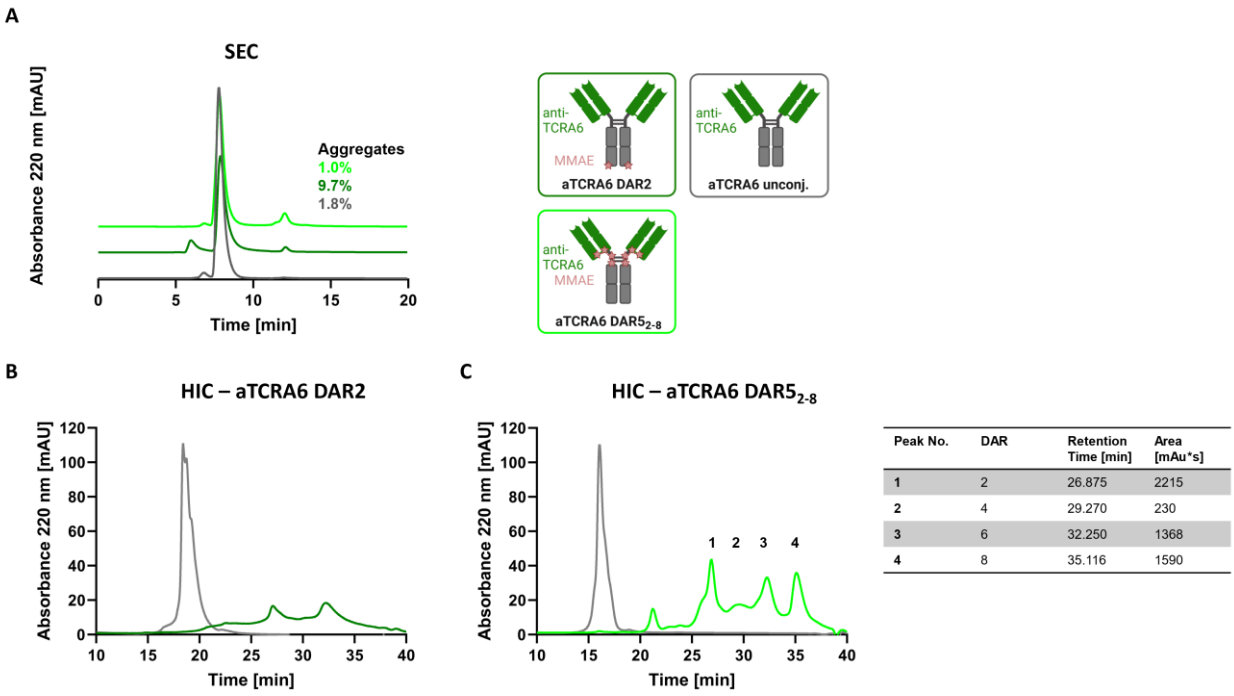


| Peak No. | DAR | Retention Time [min] | Area [mAu*s] |
|---|---|---|---|
| 1 | 2 | 26.875 | 2215 |
| 2 | 4 | 29.270 | 230 |
| 3 | 6 | 32.250 | 1368 |
| 4 | 8 | 35.116 | 1590 |

**Figure S5** Biophysical characterization of aTCRA6 DAR2 and DAR5$_{2-8}$ ADCs. (A) Size exclusion chromatography. The percentages of aggregation were determined by integration of the absorbance peak areas. (B) Hydrophobic interaction chromatography of aTCRA6 DAR2. (C) Hydrophobic interaction chromatography of aTCRA6 DAR5$_{2-8}$. The absorbance peak areas of the different species, labelled as 1-4, are depicted in the table.

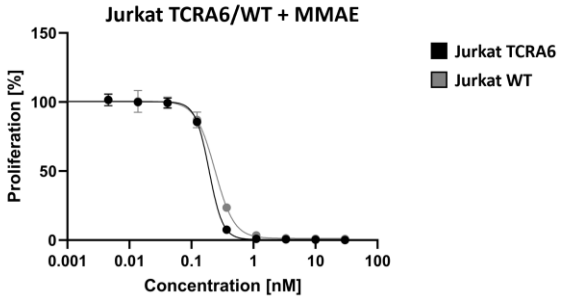


| Cell line | $EC_{50}$ | Max. lysis |
|---|---|---|
| Jurkat TCRA6 | 0.19 nM | 100% |
| Jurkat WT | 0.24 nM | 99% |

**Figure S6** Cytotoxicity of MMAE on Jurkat TCRA6 and Jurkat WT cells. Cytotoxicity was assessed by exposition of Jurkat TCRA6 target cells and Jurkat WT off-target cells to 0.005-30 nM MMAE for 72 h. Cell proliferation was normalized to untreated control cells (0 nM). $EC_{50}$s were determined using variable slope four-parameter fit. Results are shown as mean, error bars represent standard deviation derived from experimental triplicates. Data is representative of three independent experiments.

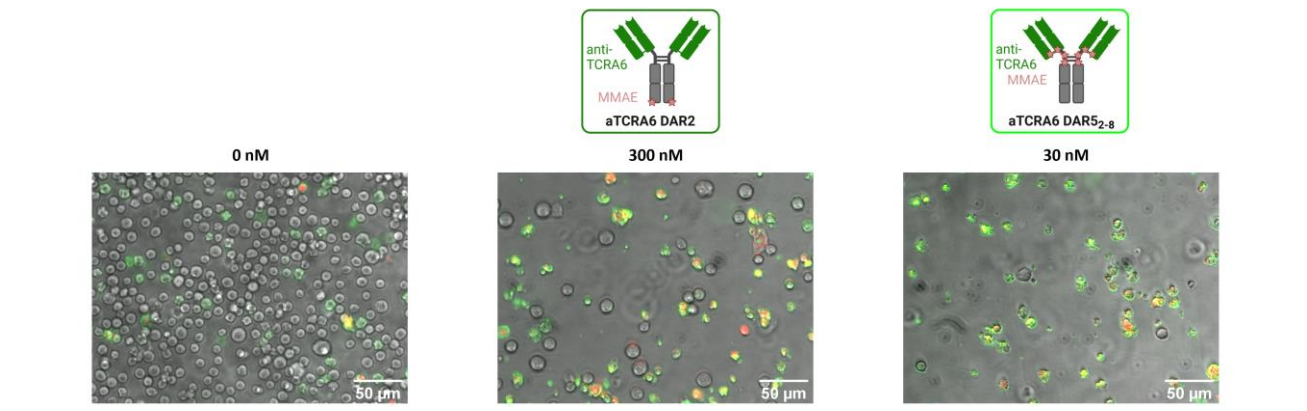


**Figure S7** Microscopic images of apoptosis induction in Jurkat TCRA6 by aTCRA6 ADC variants. Jurkat TCRA6 target cells were exposed to 300 nM aTCRA6 DAR2 and 30 nM aTCRA6 DAR5$_{2-8}$ for 72 h. Cells were stained with Annexin V-FITC (green) and propidium iodide (red) and analyzed by fluorescence microscopy. Merges of bright field and fluorescence images are depicted.

**Table S1** Amino acid sequences in one-letter code of the chimeric chicken-human aTCRA6S1 light and heavy chain. CDRs are highlighted in bold, the LAP-tag is underlined.

| | |
|---|---|
| aTCRA6S1 LC | ALTQPSSVSANLGGTVEITCS**GSSGNYYG**WYQQKSPGSAPVTVIY**YND KRPS**NIPSRFSGSKSGSTATLTITGVQAEDEAVYYCG**GFDSNYVGI**FGA GTTLTVLGQPKAAPSVTLFPPSSEELQANKATLVCLISDFYPGAVTVAW KADSSPVKAGVETTTPSKQSNNKYAASSYLSLTPEQWKSHKSYSCQVT HEGSTVEKTVAPTECS |
| aTCRA6S1 HC | AVTLDESGGGLQTPGGTLSLVCKAS**GFDFSSYLMF**WVRQAPGKGLEFI AS**ISSNDALSTDYGAAVKG**RATISRDNGQSTLRLQLNNLRAEDTGNYY CAK**SAGGWTYGHAGSIDA**WGHGTEVIVSSASTKGPSVFPLAPSSKSTS GGTAALGCLVKDYFPEPVTVSWNSGALTSGVHTFPAVLQSSGLYSLSS VVTVPSSSLGTQTYICNVNHKPSNTKVDKKVEPKSCDKTHTCPPCPAPE LLGGPSVFLFPPKPKDTLMISRTPEVTCVVVDVSHEDPEVKFNWYVDG VEVHNAKTKPREEQYNSTYRVVSVLTVLHQDWLNGKEYKCKVSNKAL PAPIEKTISKAKGQPREPQVYTLPPSRDELTKNQVSLTCLVKGFYPSDIA VEWESNGQPENNYKTTPPVLDSDGSFFLYSKLTVDKSRWQQGNVFSCS VMHEALHNHYTQKSLSLSPGK<u>GFEIDKVWYDLDA</u> |